Salisbury, M. H., Scott, J. H., et al., 1988
Proceedings of the Ocean Drilling Program, Scientific Results, Vol. 102

11. OLD OCEANIC CRUST: SYNTHESIS OF LOGGING, LABORATORY, AND SEISMIC DATA FROM LEG 102[1]

Matthew H. Salisbury,[2] James H. Scott,[3] Christian Auroux,[4] Keir Becker,[5] Wilhelm Bosum,[6] Cristina Broglia,[7] Richard Carlson,[8] Nikolas I. Christensen,[9] Andrew Fisher,[10] Joris Gieskes,[11] Mary Anne Holmes,[12] Hartley Hoskins,[13] Dan Moos,[7] Ralph Stephen,[14] and Roy Wilkens[15]

ABSTRACT

On ODP Leg 102, the *JOIDES Resolution* returned to Hole 418A at the southern end of the Bermuda Rise and logged the hole with a comprehensive suite of tools to determine the geophysical properties of old oceanic crust from *in-situ* measurements. An excellent set of density, porosity, natural gamma-ray, conductivity, resistivity, full wave and multichannel sonic (*P* and *S*), magnetic susceptibility, three-axis magnetometer, and caliper logs was obtained over varying intervals from 0 to 488 m within the basement. In addition, the sediments were logged through the pipe using the porosity and spectral gamma-ray tools, water samples were taken and temperature measurements made at selected depths in basement, and the oblique seismic experiment was successfully run with a three-component borehole seismometer clamped 41, 81, 230, 330, and 430 m within the basement.

The results demonstrate as follows:

1. Layer 2A is absent: V_p increases gradually from 4.5 km/s at the sediment/basement contact to 6.9 km/s at 1.5 km within the basement and averages 4.8 km/s in the upper 0.5 km.
2. The upper crust is anisotropic: V_p varies with azimuth by ± 0.2 km/s to a range of 0.6 km, with V_p fast parallel to spreading in the top of the section and fast subperpendicular to spreading near the bottom of the hole. In addition, the upper crust displays vertical/horizontal anisotropy, with V_p fast by 0.2 km/s in the horizontal propagation direction.
3. The upper 0.5 km of the crust is cracked at all scales of investigation because $V_{p_{lab}} > V_{p_{log}} > V_{p_{OSE}}$.
4. The average formation porosity of the section drilled is low (15%, of which 10% is grain boundary porosity and 5% is fracture porosity) but was originally higher by an amount less than or equal to the present volume of clay in the formation (9%).
5. The original formation porosity near the top of the section (Unit 5 and Subunit 8A) approached 40%; the original velocity of this interval would have been about 3.5 km/s, or that of Layer 2A.
6. The disappearance of Layer 2A was caused by infilling by an ordered sequence of alteration products formed by rock-water interaction in a closed system.

INTRODUCTION

In the middle 1970s, Houtz and Ewing (1976) recognized from seismic studies of the oceanic crust that Layer 2 could be subdivided into three layers, 2A, 2B, and 2C, on the basis of velocity (Table 1) and that the shallowest of these layers (2A) thinned and eventually disappeared with age. Because the upper levels of Layer 2 were known from dredging and shallow basement drilling to consist largely of pillow basalts, it was suggested by several authors (e.g., Schreiber and Fox, 1976) that the disappearance of Layer 2A was due to the infilling of fractures and interpillow voids by alteration products, which raised the velocity to that typical of Layer 2B.

To test this hypothesis, the Deep Sea Drilling Project (DSDP) and the Ocean Drilling Program (ODP) drilled a transect of basement holes along a flow line extending from the crest of the Mid-Atlantic Ridge, where three holes (Holes 395A, 396B, and 648B) were drilled in young crust, to the edge of the Nares Abyssal Plain, where a series of holes was drilled at Sites 417 and 418 in crust of Cretaceous age at the southern end of the Bermuda Rise (Table 2). Although none of these holes penetrated much more than 0.5 km into basement, the differences between young and old crust at the sites are striking. At the site with the youngest crust (Hole 648B), where the section consists of extremely fresh pillow basalts, the crust proved virtually undrillable because of fractures and rubble. In Holes 395A and

[1] Salisbury, M. H., Scott, J. H., et al., 1988. *Proc. ODP, Sci. Results*, 102: College Station, TX (Ocean Drilling Program).

[2] Centre for Marine Geology, Dalhousie University, Halifax, Nova Scotia B3H 3J5, Canada.
[3] U.S. Geological Survey, Denver Federal Center, Denver, Colorado 80225 (present address: James H. Scott and Assoc., 12372 W. Louisiana Avenue, Lakewood, CO 80228).
[4] Ocean Drilling Program, Texas A&M University, College Station, TX 77843.
[5] Geological Research Division, Scripps Institution of Oceanography, University of California, La Jolla, CA 92093 (present address: Rosenstiel School of Marine and Atmospheric Science, University of Miami, Miami, FL 33149).
[6] Federal Institute for Geosciences and Natural Resources, D-3000 Hannover 51, P.O. Box 51 01 53, Federal Republic of Germany.
[7] Borehole Research Group, Lamont-Doherty Geological Observatory, Columbia University, Palisades, NY 10984 (Moos, present address: Department of Geophysics, Stanford University, Stanford, CA 94305).
[8] Department of Geophysics, Texas A&M University, College Station, TX 77843.
[9] Department of Earth and Atmospheric Sciences, Purdue University, West Lafayette, IN 47907.
[10] Rosenstiel School of Marine and Atmospheric Science, University of Miami, Miami, FL 33149.
[11] Ocean Research Division, Scripps Institution of Oceanography, University of California, La Jolla, CA 92093.
[12] Department of Geology, University of Nebraska, Lincoln, NE 88588.
[13] Ocean Industries Program, Woods Hole Oceanographic Institution, Woods Hole, MA 02543.
[14] Department of Geology and Geophysics, Woods Hole Oceanographic Institution, Woods Hole, MA 02543.
[15] Earth Resources Laboratory, Massachusetts Institute of Technology, Cambridge, MA 02139 (present address: Department of Geology and Geophysics, University of Hawaii, 2525 Correa Road, Honolulu, HI 96822).

Table 1. Layered crustal velocity model of Houtz and Ewing (1976).

Layer	V_p (km/s)	Thickness (km)
2A	3.33 ± 0.10	0.74 ± 0.23
2B	5.23 ± 0.44	0.72 ± 0.26
2C	6.19 ± 0.16	[a]1.83 ± 0.75
3	6.92 ± 0.17	[b]—

[a] Cumulative thickness of Layers 2B and 2C.
[b] Thickness could not be determined from sonobuoy studies.

and 396B (7 and 10 m.y. old, respectively), although incipient alteration had clearly set in and significant penetration was readily achievable, the pillow basalts remained, in general, quite fresh, recovery was poor, and logging indicated, at least in Hole 396B, that the section drilled belonged to Layer 2A (average V_p = 3.5 km/s; Kirkpatrick, 1979).

When drilling was first undertaken in old crust on Legs 51–53 at Sites 417 and 418 (Fig. 1), it was immediately clear that the situation was very different. Whereas the basement sections drilled consisted primarily of pillow basalts as before, the basalts were strongly to profoundly altered in the upper few hundred meters of the basement: glass was completely replaced by palagonite, mafic phenocrysts and groundmass materials were extensively altered to clay, average K^+ values were high, and densities were depressed (Pritchard, 1980; Humphris et al., 1980; Pertsev and Rusinov, 1980; Juteau et al., 1980; Donnelly et al., 1980). In addition, recovery was unusually high (Table 2) and, for the first time, included significant amounts of vein material, interpillow void fillings, and annealed breccia (Pl. 1). Furthermore, the compressional-wave velocity obtained from sonic logging in the upper 100 m of Hole 417D (V_p = 4.8 km/s) and the oblique seismic experiment in the upper 250 m (V_p increases from 4.8 km/s at the top of the basement to 6.4 km/s at a depth of 1.3 km within the basement) indicated that Layer 2A was indeed absent (Stephen et al., 1980; Salisbury et al., 1980a, 1980b). It was thus concluded that the increased recovery and the disappearance of Layer 2A were due to crustal "annealing" by alteration.

Although the results at Sites 417 and 418 are impressive, operational difficulties toward the end of Leg 53 prevented logging and further drilling in Hole 418A, the deepest and most promising of the holes drilled during Legs 51–53. When Hole 418A was finally terminated at a depth of 544 m with basement, it had penetrated a complex section consisting relatively fresh massive basalts from 0–63 m in the basement (Units 1–4; Table 3), altered pillow basalts from 63 m to the base of a thick breccia unit at a depth of 186 m (Unit 5 and Subunit 6A), and a thick unit of relatively fresh pillow basalts underlain by increasingly fresh, increasingly massive pillow basalts and massive basalts (some laced with dikes) toward the bottom of the hole (Subunits/Units 6B to 16). Features of particular interest include a major polarity reversal coincident with breccia Subunit 6A (e.g., Levi 1980), increasingly steep magnetic inclinations with depth toward the base of the hole, and the recovery of with residual stress from the lower levels of the hole.

Because of its depth and high core recovery, Hole 418A was regarded as an exceptional site at which to calibrate logging equipment and to determine the geophysical properties of old crust from logging and borehole experiments. Thus, Leg 102 returned to Hole 418A after an 8-yr hiatus, cleared the hole of obstructions, and conducted the most sophisticated series of downhole experiments ever attempted in an oceanic borehole, including a two-ship seismic experiment involving the R/V *Fred H. Moore* and a seismometer lowered into the hole from the *JOIDES Resolution* and multiple lowerings of conventional and experimental logging tools provided by Schlumberger scientists from the United States and West Germany (Fig. Table 4).

GEOLOGIC SETTING

Hole 418A was drilled in 108-m.y.-old Cretaceous crust near the Vema Gap at the southern end of the Bermuda Rise. As can be seen in Figure 3, the site is located near the eastern edge of the *M0* anomaly, between two fracture zones that define the direction of spreading as N68°W. Although the region had been surveyed prior to drilling (Rabinowitz et al., 1980), a detailed survey had never been made in the immediate area of the drill holes. To rectify this situation, a series of seismic on pro-

Table 2. Basement holes on DSDP/ODP Atlantic age transect.

Hole	Leg	Location	Basement penetration (m)	Recovery (%)	Recovered lithology (%)			Age (m.y.)	Downhole experiments
					Pillow basalt	Massive basalt	Breccia		
[a,b]648B	106/109	22°55.3′N; 44°56.8′W	51	12	60	40	0	0	
[c]395A	45	22°45.35′N; 46°04.90′W	580	18	78	15	7	7	[b,d]Logging
[e]396B	46	22°59.14′N; 43°30.90′W	256	23	[f]78	[f]5	[f]17	10	[g]Logging
[h]417A	51–53	25°06.63′N; 68°02.48′W	209	61	75	9	16	108	
[h]417D	51–53	25°06.69′N; 68°02.82′W	366	72	71	24	5	108	[i]Logging, [j]oblique seismic experiment
[k]418A	51–53	25°02.10′N; 68°02.82′W	544	72	69	27	4	108	[l]Logging, oblique seismic experiment
[k]418B	51–53	25°02.08′N; 68°03.45′W	10	74	100	0	0	108	

[a] A. Adamson, pers. comm., 1987.
[b] Leg 109 Shipboard Scientific Party, 1986.
[c] Shipboard Scientific Party, 1979a.
[d] Hyndman, Salisbury, et al., 1984.
[e] Shipboard Scientific Party, 1979b.
[f] Based on Units 1–5.
[g] Kirkpatrick, 1979.
[h] Shipboard Scientific Parties, 1980a.
[i] Salisbury et al., 1980a.
[j] Stephen et al., 1980.
[k] Shipboard Scientific Parties, 1980b.
[l] Shipboard Scientific Party, 1986.

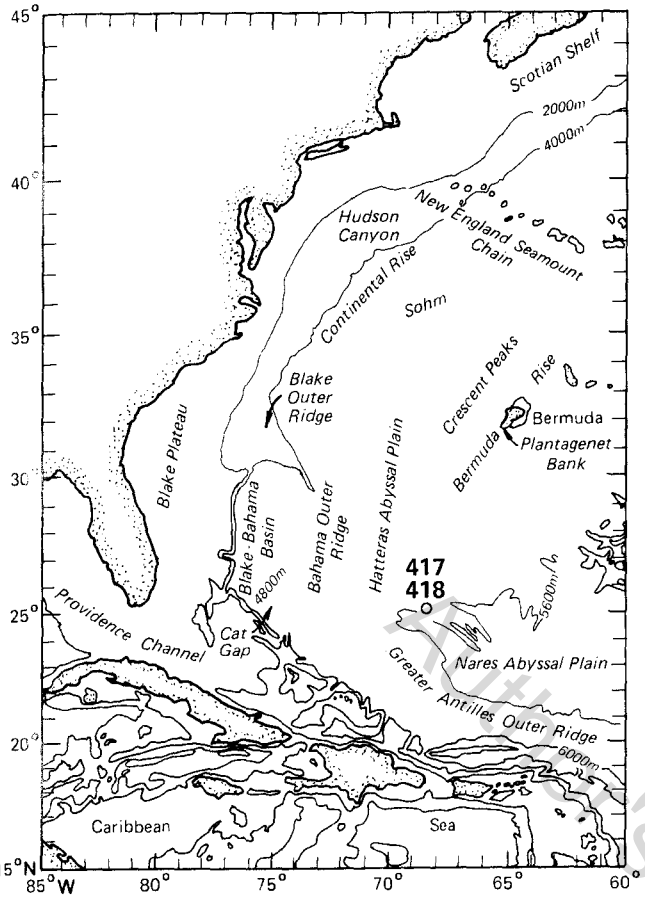

Figure 1. Location of Sites 417 and 418.

files was run from the *Moore* along grid lines covering a square-shaped area, with sides of about 16 km, centered on Hole 418A (Fig. 4) while waiting for the geophysical logging of Hole 418A to be completed aboard the *JOIDES Resolution*.

The profiles indicate that the hole is located on the eastern edge of an irregularly shaped, bedrock valley (Fig. 5) trending approximately N20°E and filled with over 300 m of sediments. Relief on the basalt bedrock surface is strong, with dips as great as 14%. The seafloor terrain generally follows the pattern of the basalt surface, but with muted relief and maximum dips of only 5% or so. A reflector within the sediments is believed to represent the top of the middle Eocene (Unit III).

SEISMIC VELOCITY STRUCTURE OF THE CRUST

During the original drilling operations in 1977, an oblique seismic experiment (OSE) was conducted in Hole 417D to study the seismic velocity structure around the drill site and to determine whether seismic anisotropy is present in the upper levels of the crust. Because of drilling and instrument problems (the lower part of the hole was blocked by pipe; only the vertical component of the borehole seismometer could be made to operate), the experiment was not as comprehensive as originally planned. Nonetheless, the excellent data obtained showed that anisotropy was present in the upper levels of the hole and that compressional- and shear-wave velocities increased from V_p = 4.6 and V_s = 2.6 km/s at the top of the basement to values typical of Layer 3 (6.8 and 3.6 km/s, respectively) at a depth of between 1.5 and 1.6 km (Stephen et al., 1980; Stephen and Harding, 1983).

On Leg 102, a much more extensive OSE was successfully conducted with the *Moore* providing a series of explosive and air gun shots in a pattern of radial and concentric lines centered on Hole 418A (Swift and Stephen, this volume). A three-component geophone was clamped at five different depths ranging from 41 to 430 m within the basement. The shooting patterns, which were different for different geophone depths, are shown diagrammatically in Figure 6, and typical ray paths are shown in Figure 7.

The data from the OSE were reduced in three ways. In the simplest, vertical seismic profile (VSP) treatment, interval velocities were calculated from vertical incidence traveltimes with the seismometer clamped 81, 230, 330, and 430 m within the basement. This gives accurate compressional-wave values for a vertical propagation path in the immediate vicinity of the borehole (Table 5A).

In a second approach, the inflection point method (Stephen and Harding, 1983) was used to determine compressional-wave velocities at the seismometer clamp points from the radial shooting lines. The velocities calculated by this means (Table 5B) represent *P*-wave velocities for subhorizontal propagation paths sampling a large volume of rock in the vicinity of the hole. Values were calculated both before and after reduction to basement, but the former values are preferred because they are consistent with observed traveltimes.

In the third approach, compressional-wave velocities were determined using $\tau - \zeta$ inversion (Dorman and Jacobson, 1981). This technique allows compressional-wave velocities to be determined to depths considerably greater than that of the borehole (Table 5C), again for relatively long subhorizontal propagation paths. Shear-wave velocities were then calculated from the compressional-wave data assuming

$$V_s = 0.55V_p. \quad (1)$$

Although not rigorously determined, the shear-wave velocities derived by this means would appear to be approximately correct, because synthetic seismograms generated from these values using the reflectivity method (Fuchs and Müller, 1971) are consistent with observed OSE data (e.g., Fig. 8).

Finally, traveltimes from the circular shooting lines to the borehole receiver were analyzed to determine anisotropy vs. range and depth. Pronounced *P*-wave anisotropy (±0.22 km/s) was observed at Site 418 (Fig. 9) in the upper 0.5 km of the basement and within 0.6 km of the hole but was absent at greater depths and ranges. Curiously, the fast direction for V_p is parallel to spreading in the upper levels of the hole but becomes subperpendicular at depth.

As can be seen in Figure 10, subtle differences in *P*-wave velocity result from different reduction techniques. The $\tau - \zeta$ and inflection (before reduction to basement) methods are in excellent agreement, giving average velocities (V_p) in the upper 0.5 km of 4.8 km/s, but both give higher average velocities than the VSP method (4.63 km/s). If this difference is real, then the upper crust is anisotropic to at least 430 m with V_p fast in the horizontal direction, as suggested by Newmark et al. (1985) for Hole 504B on the basis of borehole televiewer data. Regardless of anisotropy and however reduced, the *P*-wave velocities obtained by the OSE equal or exceed 4.5 km/s at the top of the basement and increase with depth to values typical of Layer 3 at a depth of about 1.5 km. This is in excellent agreement with the OSE results at Site 417 and confirms that Layer 2A is absent.

WELL LOGGING

Following the initial pipe lowerings for temperature measurements and water sampling, pipe was run 488 m into the basalt to clear the hole of bridges and then raised to 42 m above the basalt/sediment contact, after which a full suite of conventional and experimental well logs was run in the borehole. The conventional logs were run by Schlumberger and included sonic (*P*-

Table 3. Basement lithologic units, Hole 418A, from results of Legs 52 and 53 (Shipboard Scientific Parties, 1980b).

Unit/ subunit	Depth[a] below seafloor (m)	Depth[a] in basement (m)	Thickness (m)	Type of cooling unit	Phenocryst assemblage[b]	Interval (core, section, cm)
1	324.0-329.6	0-5.6	5.6	Pillow basalt	Plag-(Oliv)	15-1, 20 to 16-1, 10
2A	329.6-331.7	5.6-7.7	2.1	Massive basalt	Plag-(Oliv)	16-1, 10 to 16-2, 105
2B	331.7-339.0	7.7-15.0	7.3	Massive basalt	Plag-(Oliv)	16-2, 105 to 17-4, 150
2C	339.0-363.1	15.0-39.1	24.1	Massive basalt	Plag-(Oliv)	18-1, 0 to 20-5, 81
2D	363.1-376.6	39.1-52.6	13.5	Massive basalt	Plag-(Oliv)-[Cpx]	20-5, 81 to 24-1, 57
3	376.6-383.3	52.6-59.3	6.7	Pillow basalt	Plag-(Oliv)-[Cpx]	24-1, 57 to 25-2, 60
4	383.3-387.1	59.3-63.1	3.8	Massive basalt	Plag-(Oliv)-[Cpx]	25-2, 60 to 26-2, 110
5	387.1-498.5	63.1-174.5	111.4	Pillow basalt and breccia	Plag-(Oliv)-[Cpx]	26-2, 110 to 40-3, 47
6A	498.5-510.5	174.5-186.5	12.0	Breccia	Plag-Oliv-(Sp)-[Cpx]	41-1, 0 to 42-2, 150
6B	510.5-611.0	186.5-287.0	100.5	Pillow basalt	Plag-Oliv-(Sp)-[Cpx]	42-3, 0 to 53-3, 150
7	611.0-629.2	287.0-305.2	18.2	Pillow basalt	Plag-Oliv-Cpx	54-1, 0 to 55-7, 70
8A	629.2-632.9	305.2-308.9	3.7	Pillow basalt	Plag-Oliv-Cpx	55-7, 70 to 56-3, 45
8B	632.9-636.3	308.9-312.3	3.4	Massive(?) basalt	Plag-Oliv-Cpx	56-3, 45 to 56-5, 125
8C	636.3-671.8	312.3-347.8	35.5	Pillow basalt	Plag-Oliv-Cpx	56-5, 125 to 60-4, 33
9	671.8-676.5	347.8-352.5	4.7	Massive, vesicular basalt	Plag	60-4, 33 to 60-6, 66
10	676.5-686.0	352.5-362.0	9.5	Massive basalt	Plag	61-1, 0 to 61 bit, 95
11	686.0-695.5	362.0-371.5	9.5	Pillow basalt	Plag-Cpx-Oliv	62-1, 0 to 63-5, 119
12	695.5-698.2	371.5-374.2	2.7	Massive(?) basalt	Plag-Cpx-Oliv	64-1, 0 to 64-2, 122
13	698.2-786.5	374.2-462.5	88.3	Pillow basalt and breccia	Plag-Cpx-Oliv	64-2, 122 to 75-4, 150
14A	786.5-793.6	462.5-469.6	7.1	Massive basalt	Plag-Cpx-Oliv	75-5, 0 to 77-1, 50
14B	793.6-821.5	469.6-497.5	27.9	Massive basalt	Plag-Cpx-Oliv	77-1, 50 to 79-7, 124
14C	821.5-859.8	497.5-535.8	38.3	Massive basalt	Plag-Cpx-Oliv	80-1, 0 to 86-1, 25
15A	[c]—	—	—	Basalt dikes	Plag-Oliv-Cpx	79-1, 75 to 79-1, 110 79-2, 78 to 79-1, 105 79-3, 105 to 79-4, 95
15B	—	—	—	Basalt dikes	Plag-Oliv	80-2, 117 to 80-3, 127 80-4, 2 to 80-4, 42 80-4, 107 to 80-5, 110
16	859.8-868.0	535.8-544.0	8.2	Pillow basalt and breccia	Plag-Oliv-Cpx-Sp	86-1, 25 to 86-6, 55

[a] Depths corrected for spacers.
[b] Plag = plagioclase; Oliv = olivine; Cpx = clinopyroxene; Sp = spinel.
[c] Undetermined.

and full wave), induction and spherically focused resistivity, natural and spectral gamma-ray, gamma density, neutron porosity, and caliper logs. The experimental logs were run by the Bundesanstalt für Geowissenschaften und Rohstoffe (BGR) of the Federal Republic of Germany, the United States Geological Survey, and Lamont-Doherty Geological Observatory and included magnetic field, magnetic susceptibility, and multichannel sonic logs. Most of the logs were run from near the top of the basement to a depth of 460 m or more within the basement, passing through most of the lithologic sequence drilled on Legs 51-53 (Table 3). The Schlumberger spectral gamma-ray and neutron porosity logs were run in the sediments above the basalts, but these measurements were somewhat degraded because they had to be made through the drill pipe to avoid problems of caving and bridging. The uppermost section of the susceptibility log extends 30 m into the sediments. Figure 2 shows the depth intervals covered by all of the logs, and Table 4 gives information on how the logs were run, along with an indication of the relative quality of the data. Figure 11 shows a selection of the most important logs together with lithology. Table 6 presents a summary of the properties of the basement section for lithologic Subunits/Units 1-13C based on these logs, and Table 7 gives the average corrected formation properties for the three major depth intervals logged in Hole 418A (Broglia and Moos, this volume).

As expected, an examination of Table 7 shows a positive correlation between total formation porosity and natural gamma radiation and a negative correlation between porosity and density, velocity, resistivity, and susceptibility. Many other features, however, are unusual; the average formation velocity at Site 418 is high (V_p = 5.07 km/s), as is the formation density (2.6 g/cm^3), whereas the porosity is low (15%). Furthermore, the natural gamma radioactivity is high, especially in the upper levels of the section (23 GAPI units in Unit 5-Subunit 6A). Using the relationship between natural gamma radiation and clay content in cores, Broglia and Moos (this volume) computed a clay log that shows clay constitutes nearly 20% of the rock in Unit 5 and Subunit 6A but is an order of magnitude less at greater depths in the hole. From the clay and velocity logs, they were able to estimate primary and secondary (fracture) porosity vs. depth and to demonstrate that the upper 0.5 km of the crust at Site 418 is about 10% primary porosity and 5% cracks by volume, in excellent agreement with earlier estimates from logging at Site 417 (Salisbury et al., 1980a).

The 12-channel full waveform log obtained in the lower section of the hole between 469 and 788 m provided high-quality *P*-wave data that generally confirmed the validity of the Schlumberger sonic log (*P*-wave) and also provided excellent *S*-wave data. However, the average *P*- and *S*-wave velocities obtained (5.5 and 2.9 km/s, respectively) are generally higher than velocities obtained for the same interval and propagation direction with the borehole seismometer (Fig. 10), suggesting that the latter senses cracks that lie beyond the borehole wall and thus, are not seen by the sonic-logging tools.

As expected, the logs obtained with the three-axis magnetometer and the magnetic susceptibility tool (Bosum and Scott, this volume) were consistent with data obtained from the cores on Legs 51-53 (e.g., Levi et al., 1980). The magnetometer, which is gyroscope-stabilized, picked up the magnetic field reversal seen in core samples above breccia Subunit 6A at 180 m within the basement and measured a Cretaceous pole position consis-

tent with the age of the site (the first such determination ever made in oceanographic research).

In addition to determining formation properties from logs as a function of depth for crustal studies, it was recognized that Hole 418A, with its high core recovery, provided an unusual opportunity to study logging tool responses in a variety of mafic rock types. Figure 12 shows the average values and statistical ranges (± 1 standard deviation) of the properties obtained by the density, neutron porosity, velocity (V_p from long-spaced sonic), resistivity (spherically focused log), radioactivity (natural gamma-ray), and magnetic susceptibility tools for breccias (Subunit 6A), altered pillow basalts (Unit 5), "fresh" pillow basalts (Subunits/Units 6B, 7, 8B, 8C, 11, 13A, and 13C), massive vesicular basalt (Unit 9), and massive basalt (Subunits/Units 8B, 10, 12, and 13B). The upper massive basalts (Subunits 2A–2D and Unit 4) were excluded from the averages because density logs were not available in these intervals.

Figure 12 shows that the average values and ranges of density, velocity, resistivity, and susceptibility tend to increase and that the averages and ranges of porosity and radioactivity tend to decrease with decreasing fracturing and alteration. These relationships, though based on a limited data set, suggest that it may be possible to differentiate between different basaltic rock types (massive, altered pillows, breccia, etc.) by running statistical analyses on well-log and core data from a well-characterized hole and then using the results to predict rock type as a function of a suite of well-log values and the statistical relationships established. In addition, it may be possible to determine, at least semiquantitatively, the degree of fracturing and alteration associated with the various rock types. Now that the DSDP/ODP data base of well-log and lithologic information on oceanic basalts is fairly large and of rather high quality, it might be appropriate to investigate these possibilities further by testing the validity and accuracy of identifying rock type and rock character by computer. Such an approach would be particularly useful for establishing lithology-depth relationships where core recovery is poor.

COMPARISON OF LABORATORY, LOG, AND SEISMIC DATA

During the course of Legs 51–53 and the follow-up laboratory studies on samples from Holes 417D and 418A, a vast amount of information was gathered on the physical properties of samples from old oceanic crust (Shipboard Scientific Parties, 1980a, 1980b; Hamano, 1980; Christensen et al., 1980; Johnson, 1980). This and the logging data are summarized in Table 7, and individual values of compressional-wave velocity, wet-bulk density, and porosity measured at atmospheric pressure on samples from Hole 418A are superimposed on the corrected logs in Figure 13 (Broglia and Moos, this volume). Though the agreement between laboratory and logging data is much better than is commonly observed in oceanic crust (see, for example, Kirkpatrick, 1979) and is excellent in selected units (for example, massive basalt Units 2 and 10), the logging velocities and densities are generally lower and the porosities higher than laboratory values. This indicates, as does the seismic anisotropy detected by the OSE, that cracks still exist.

Because of the number and quality of velocity studies conducted in the borehole and on samples from the core, Hole 418A presents an unusual opportunity to compare compressional- and shear-wave velocities determined under *in-situ* conditions at a variety of scales of investigation. To facilitate such a comparison, shear-wave velocities were measured on 12 samples from Hole 418A at hydrostatic confining pressures ranging from 0.1 to 2.0 kbar. These data, plus compressional-wave velocities measured after Legs 51–53 in the same laboratory on these and other samples from Hole 418A, are presented in Table 8 and plotted vs. depth in Figure 14 at an estimated differential confining pressure of 0.1 kbar. From this figure it is clear that the compressional- and shear-wave velocities of the rocks themselves increase steadily with depth at rates of

$$V_p = 1.91z + 5.25 \quad (2)$$

$$V_s = 2.00z + 2.56, \quad (3)$$

where velocities are in km/s and z is the depth in km. Although the trends are clear, it should be pointed out that the values of V_p and V_s will be higher if lithostatic or hydrostatic conditions prevail. Figure 15 shows, however, that the range of possible velocities for any given sample is small for the range of pressure conditions possible at Site 418 ($P = P_{differential}$ to $P_{hydrostatic}$; i.e., P = 0.1 to 1.0 kbar).

It becomes clear from cross-plotting V_p and V_s values determined from multichannel sonic logging (Fig. 16), instead of cross-plotting laboratory values of compressional-wave velocity against shear-wave velocity, that the major lithologies encountered in the upper levels of the crust occupy distinct formation velocity (V_p-V_s) fields: the massive basalt units cluster around 6.0 and 3.4 km/s for V_p and V_s, respectively; breccias cluster at the low end of the velocity spectrum (4.6 and 2.5 km/s, respectively); and pillow basalts occupy a broad field in between. Thus, logging velocities can be used to distinguish rock type. Furthermore, because the matrix petrology is (almost) invariant, the velocity trajectories are controlled by porosity. Formation porosity can be determined from velocity from the relation

$$\phi = 95.6 - 15.4V_p, \quad (4)$$

where ϕ is in % and V_p is in km/s (Broglia and Moos, this volume).

What is more surprising, however, is that the ranges and trajectories of compressional- and shear-wave velocities determined from laboratory studies, logging, and seismic experiments at Site 418 coincide (Fig. 16), a phenomenon that we attribute to the disappearance of low aspect ratio cracks in old crust. Although the ranges of velocities determined at different scales of investigation may coincide, it is nonetheless clear from Figures 10 and 16 and Table 9 that the averages do not. Because the velocities decrease with increasing scale of investigation for the same propagation directions, some cracks remain at all scales even though Layer 2A is absent.

ALTERATION

On Legs 51–53, it was recognized from whole-rock geochemical analyses of representative core samples that the upper levels of the basement at Sites 417 and 418 were strongly altered, with K_2O averaging 0.5% (Fig. 17; Flower et al., 1980) in Unit 5 and Subunit 6A, a value qualitatively confirmed by logging on Leg 102. From thin-section, scanning electron microscope (SEM), and X-ray diffraction (XRD) analysis, Humphris et al. (1980), Pritchard (1980), Pertsev and Rusinov (1980), and Holmes (this volume) have demonstrated that the increase in K is associated with the presence of alteration products, with about 40% of the natural gamma-ray count being due to potassium feldspar, 25%–50% to palagonite, and 10%–33% to K-rich clays; thus, the rock in these units consists of approximately 24% K-spar, 25% palagonite, and 3% K-rich clay (10% in the breccias of Subunit 6A). Assuming that the K resides largely in clay and that all of the alteration products now observed fill pre-existing voids (fractures, interpillow voids), Broglia and Moos (this volume) estimated that the average original porosity of the upper levels of the crust at Site 418 was as much as 40%. From equation 4, this implies that the velocity, V_p, of the upper crust before alteration

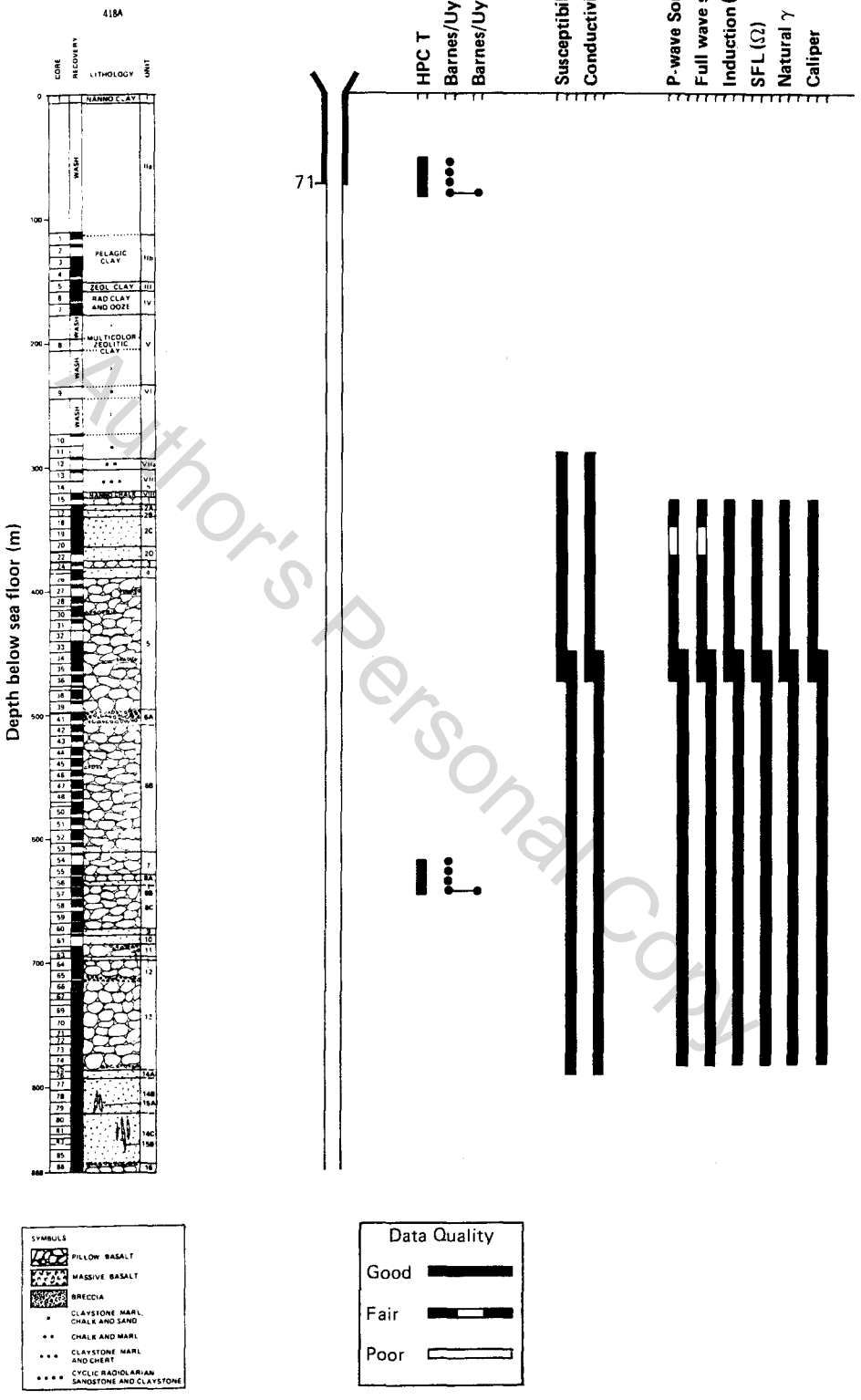

Figure 2. Leg 102 downhole operations summary, Hole 418A (Shipboard Scientific Party, 1986).

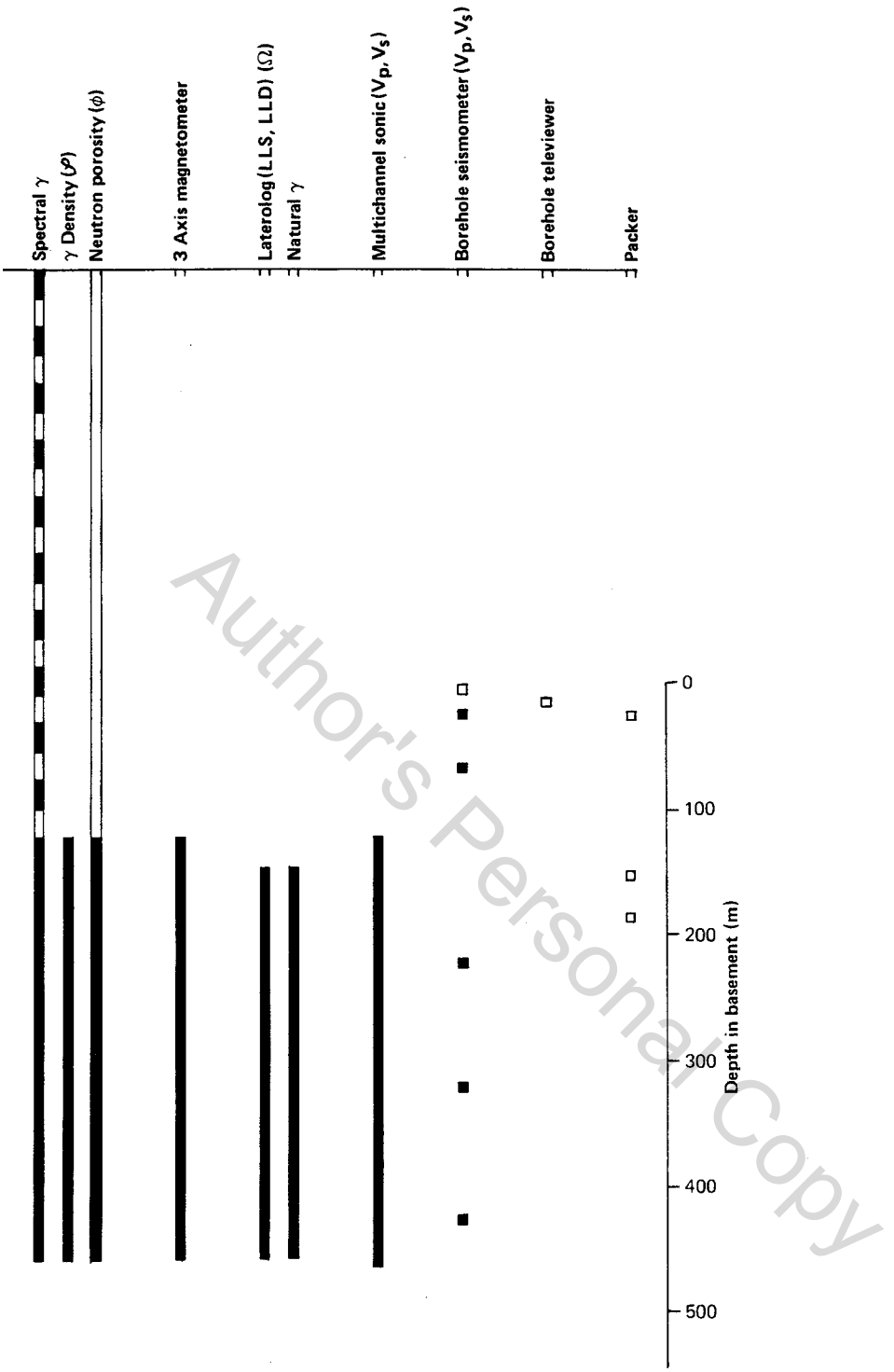

Figure 2 (continued).

Table 4. Leg 102 downhole operations summary, Hole 418A (Shipboard Scientific Party, 1986).

Run	Date	Time (hr)	Depth below rig floor (m)	Depth below seafloor (m)	Depth in basement (m)	Logging direction	Tool/test	Data quality	Remarks
HPC temperature probe-Barnes/Uyeda temperature probe-water sampler									
1	3/24/85	2145–2400	[a]5571–5600	52–81	–	Down	HPC temperature	Good	
							Uyeda temperature	Good	
	3/25/85	0000–0300					Barnes water sampler	Good	Sampled at 81 mbsf
2	3/26/85	0330–0645	[a]6143–6167	624–649	300–325	Down	HPC temperature	Good	
							Uyeda temperature	Good	
							Barnes water sampler	Good	Sampled at 649 mbsf
USGS magnetic susceptibility tool									
1	3/26/85	1625–2400	[b]5805–5847	295–337	0–12	Down	Susceptibility	Good	Tool temperature too
	3/27/85	0000–0320					Conductivity	Poor	low
2	3/27/85	0535–1200	[b]5831–5990	321–480	0–156	Down, up	Susceptibility	Good	Tool temperature too
							Conductivity	Poor	low ([illegible] only)
Downhole logging									
1	3/27/85	1245–2130	[b]5837–5990	327–480	3–156	Up	Vp	Good	
							Sonic waveform	Good	
							ILM	Good	
							ILD	Good	
							SFL	Good	
							γ	Good	
							Caliper		
2	3/28/85	0330–1115	[b]5968–6298	458–788	134–464	Down, up	Vp	Good	
							Sonic waveform	Good	
							ILM	Good	
							ILD	Good	
							SFL	Good	
							γ	Good	
							Caliper	Good	
								Good	
3	3/28/85	1115–2100	[b]5510–5972	0–462	0–138	Up	Spectral γ	Fair	Through pipe
			5972–6300	462–790	138–466	Down, up		Good	
			5510–5972	0–462	0–138	Up	γ-density	Poor	Through pipe
			5972–6300	462–790	138–466	Down, up		Good	
			5510–5972	0–462	0–138	Up	Neutron porosity	Poor	Through pipe
			5972–6300	462–790	138–466	Down, up		Good	
German three-axis magnetometer									
1	3/28/85	2100–2400	[b]5975–6300	465–790	141–466	Down, up	$H_{x,y,z}$	Good	
	3/29/85	2400–1500							
Downhole logging									
4	3/29/85	1500–2345	[b]6000–6295	490–785	166–461	Up	Ω Laterolog LLS	Good	
							LLD	Fair	Out of calibration
LDGO multichannel sonic tool									
1	3/30/85	0100–0745	[b]5875–6310	365–800	41–476	Down, up	Vp, Vs	Good	
USGS magnetic susceptibility tool									
3	3/30/85	0745–1600	[b]5975–6310	465–800	141–476	Down, up	Susceptibility	Good	Tool temperature too
							Conductivity	Poor	low ([illegible])
WHOI borehole seismometer									
1	3/30/85	1815–2400	[b]6065, 6165,	555, 655,	230, 330,	Stationary	Vp, Vsv, Vsh	Good	Shooting conducted
	3/31/85	0000–2400	6265	755	430		Anisotropy		by *Moore*
	4/1/85	0000–2400							
	4/2/85	0000–2400							
	4/3/85	0000–2400	5853, 5876,	343, 366,	18, 41,	Stationary	Evanescent waves	Good	Cable failed at
	4/4/85	0000–0430	5916	406	81				5853-m position
Packer									
1	4/6/85	1625–2400	[b]5867, 5985,	347, 465,	23, 141	Stationary	Pore pressure,	—	Packer would not
	4/7/85	0000–0930	6037	517	193		permeability		seat
LDGO borehole televiewer									
1	4/7/85	1200–2300	[b]5870	360	36	Down	Borehole imagery	Fair	Slow sweep; tool
							Acoustic caliper	Fair	caught on ledge

[a] Subtract 10 m to obtain depth below sea level.
[b] Equals depth below sea level (rig floor height and cable stretch cancel each other, by coincidence).

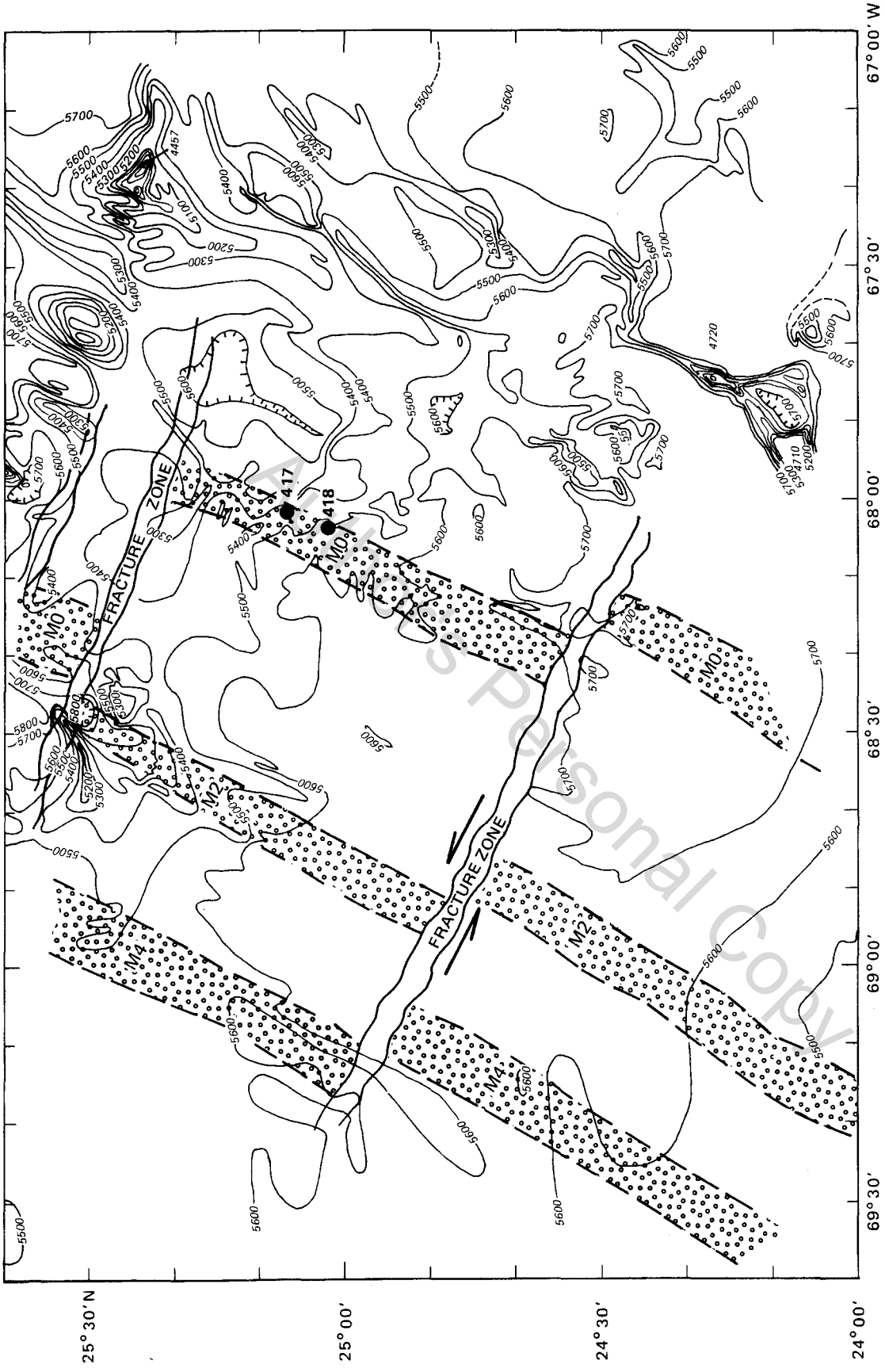

Figure 3. Bathymetry and positions of magnetic source bodies near Sites 417 and 418 (Rabinowitz et al., 1980). Depths contoured in 100-m intervals.

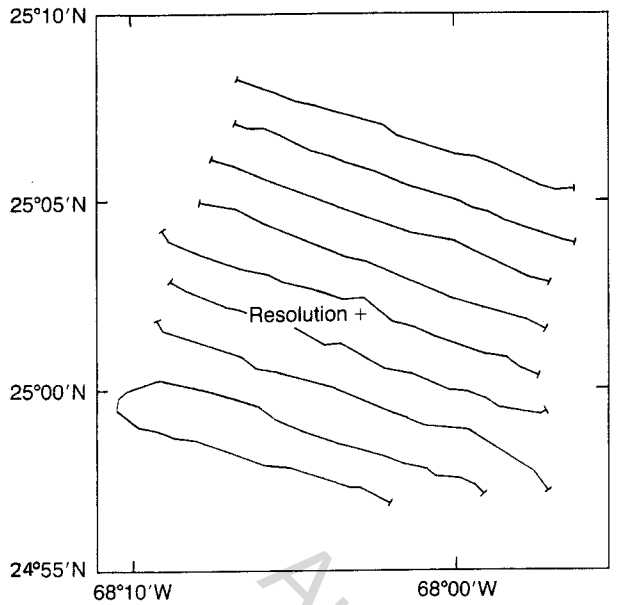

Figure 4. Location of seismic reflection lines run by R/V *Fred H. Moore* during Leg 102.

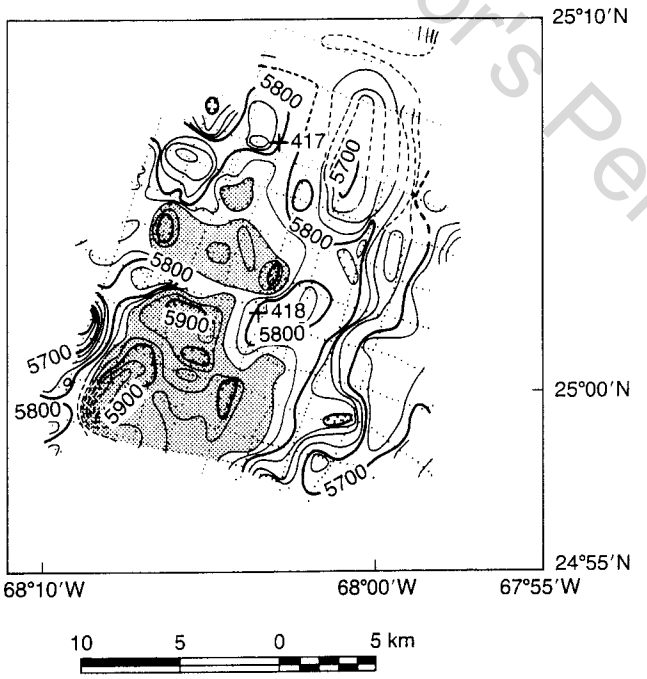

Figure 5. Basement topography showing valley (stippled) near Sites 417 and 418 (crosses). Contours in 25-m intervals. Figure after Senske and Stephen (this volume).

was less than 3.5 km/s (Fig. 18) (i.e., that Layer 2A was present when this crust resided at the ridge crest). Although the estimates of original porosity and velocity are only qualitative (if some of the K resides in K-spar, the original large-scale porosity would be lower; if K-poor alteration products such as calcite, quartz, and K-poor clays are abundant, the porosity was higher), they nonetheless appear to be approximately correct.

If infilling has occurred on the scale implied by the logging data, it should be observable in the core. This is indeed the case:

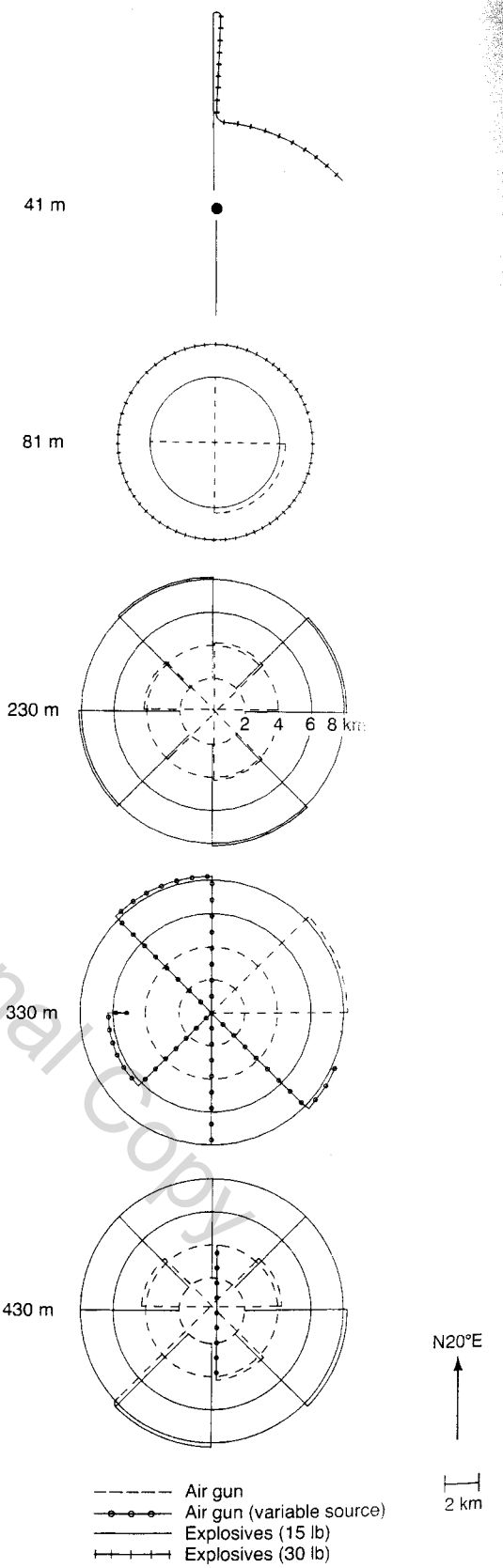

Figure 6. Air gun and explosive shooting patterns conducted in the vicinity of the *JOIDES Resolution* during oblique seismic experiment. Seismometer clamp points given in m within the basement for each shot pattern. Figure after Shipboard Scientific Party (1986).

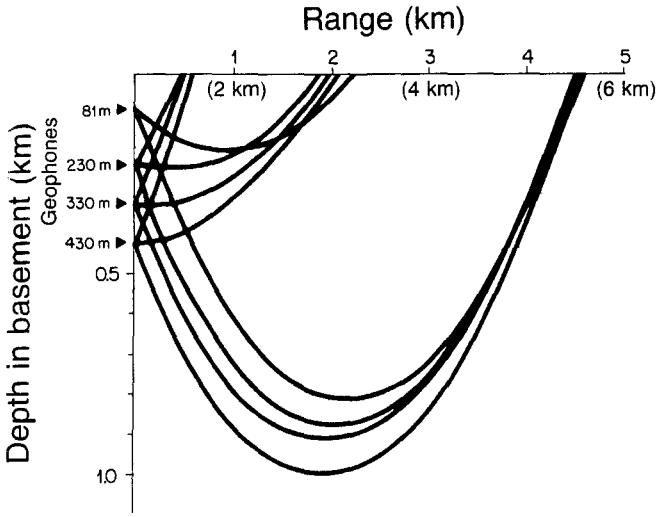

Figure 7. Typical ray paths in basement for circular shooting patterns with 2-, 4-, and 6-km radii. 4:1 vertical exaggeration.

Table 5A. Interval velocities from vertical seismic profiling.

Depth in basement (m)	V_p (km/s)
0–81	—
81–230	4.6
230–330	4.5
330–430	4.8
mean	4.6

Table 5B. Inflection point velocities from fits to radial line data (after Swift and Stephen, this volume).

Depth in basement (m)	Data processing	Number of shots	Inflection point range (km)	V_p (km/s)
41	Before reduction	24	2.43	4.71
	After reduction	24	—	5.09
81	Before reduction	119	3.18	4.63
	After reduction	—	—	—
230	Before reduction	294	3.95	4.92
	After reduction	302	2.45	4.67
330	Before reduction	245	3.73	4.93
	After reduction	284	2.35	4.59
430	Before reduction	305	4.55	5.03
	After reduction	305	2.59	4.79

breccias are typically sealed with clays, interpillow voids with palagonite, and veins and vesicles with ordered sequences of oxides, clays, pyrite, and calcite (Pl. 1; Shipboard Scientific Parties, 1980a, 1980b). On the basis of SEM and XRD transects across these sequences, Holmes (this volume) concluded that the alteration products evolved continuously in a closed system. The first stage of alteration involved oxidation and the precipitation of Fe oxide-hydroxides on the walls of veins and vesicles. This was followed in turn by the precipitation of K-rich clays (celadonite, celadonite/nontronite, or K-rich nontronite) from the least-evolved fluid; by increasingly K-poor, Mg-rich clays and eventually saponite and pyrite as the pore fluid evolved from a K- and Fe^{3+}-rich to a K-poor, Mg-, Fe^{2+}-, Al-, and Ca-rich fluid; and, eventually, by calcite as the CO_2 level increased. In the upper levels of the section (Unit 5 and Subunit 6A) and parts of Subunits/Units 8B–13A, a second oxidizing stage, initiated perhaps by off-axis faulting, caused saponite to alter to iddingsite, releasing silica, and plagioclase to alter to K-spar, releasing Ca. The products of this last stage of alteration thus include Fe oxide-hydroxides, iddingsite, K-spar, quartz, and calcite.

Table 5C. Results of $\tau - \zeta$ inversion (after Swift and Stephen, this volume).

Depth in basement (km)	V_p (km/s)	$V_s = 0.55V_p$ (km/s)
0.0	4.545	2.50
0.637 ± 0.091	5.342	2.94
0.770 ± 0.084	5.580	3.07
1.551 ± 0.113	6.849	3.77

The final consequences of the alteration processes described in this section would be a change from convective to conductive heat flow in response to decreasing permeability and an equilibrium pore-fluid chemistry showing a marked enrichment in Ca and Si and a depletion in K with respect to seawater. These predictions were confirmed by borehole temperature and pore-fluid chemistry measurements conducted during Leg 102 (Shipboard Scientific Party, 1986; Gieskes et al., this volume).

CONCLUSIONS

Upon the completion of drilling operations at Sites 417 and 418 on Legs 51–53, it was concluded that the properties of old oceanic crust were very different from young crust because of alteration and infilling of void space with age. Because these conclusions were based on a suite of geophysical logs that was limited to the upper 93 m of basement in Hole 417D, plus visual and laboratory studies of the core, they could only be regarded as tentative.

On Leg 102, Hole 418A, the deepest of the holes originally drilled in the area, was reentered and logged to a depth of 0.5 km into the basement using an extensive suite of state-of-the-art logging tools. The original conclusions were confirmed and a number of important findings were made concerning the geophysical properties of old oceanic crust:

1. Layer 2A is absent. From the results of the OSE at Site 418, it is clear that V_p increases gradually from 4.5 km/s at the top of the basement to velocities typical of Layer 3 (6.9 km/s) at a depth of 1.5 km within the basement, whereas V_s increases from 2.4 to 3.7 km/s over the same interval.

2. The upper 0.5 km of the crust displays azimuthal anisotropy to a range of about 0.6 km. V_p varies with azimuth by ±0.2 km/s, with the fast direction lying parallel to spreading in the upper levels of the crust but rotating counterclockwise with depth until it is subperpendicular to spreading at a depth of about 0.5 km.

3. The upper 0.5 km of the crust displays vertical/horizontal anisotropy with V_p fast in the horizontal direction (4.8 km/s by $\tau - \zeta$ and inflection point analysis) and slow in the vertical direction (4.6 km/s by VSP analysis).

4. Although less pervasively cracked than young crust, the upper 0.5 km of the basement at Site 418 is nonetheless cracked at all scales of investigation. This is a necessary consequence of the preceding three conclusions, and the fact that the average compressional-wave velocity of samples from this interval (5.7 km/s) is greater than the interval velocity determined from logs (5.1 km/s), which, in turn, is greater than that determined from

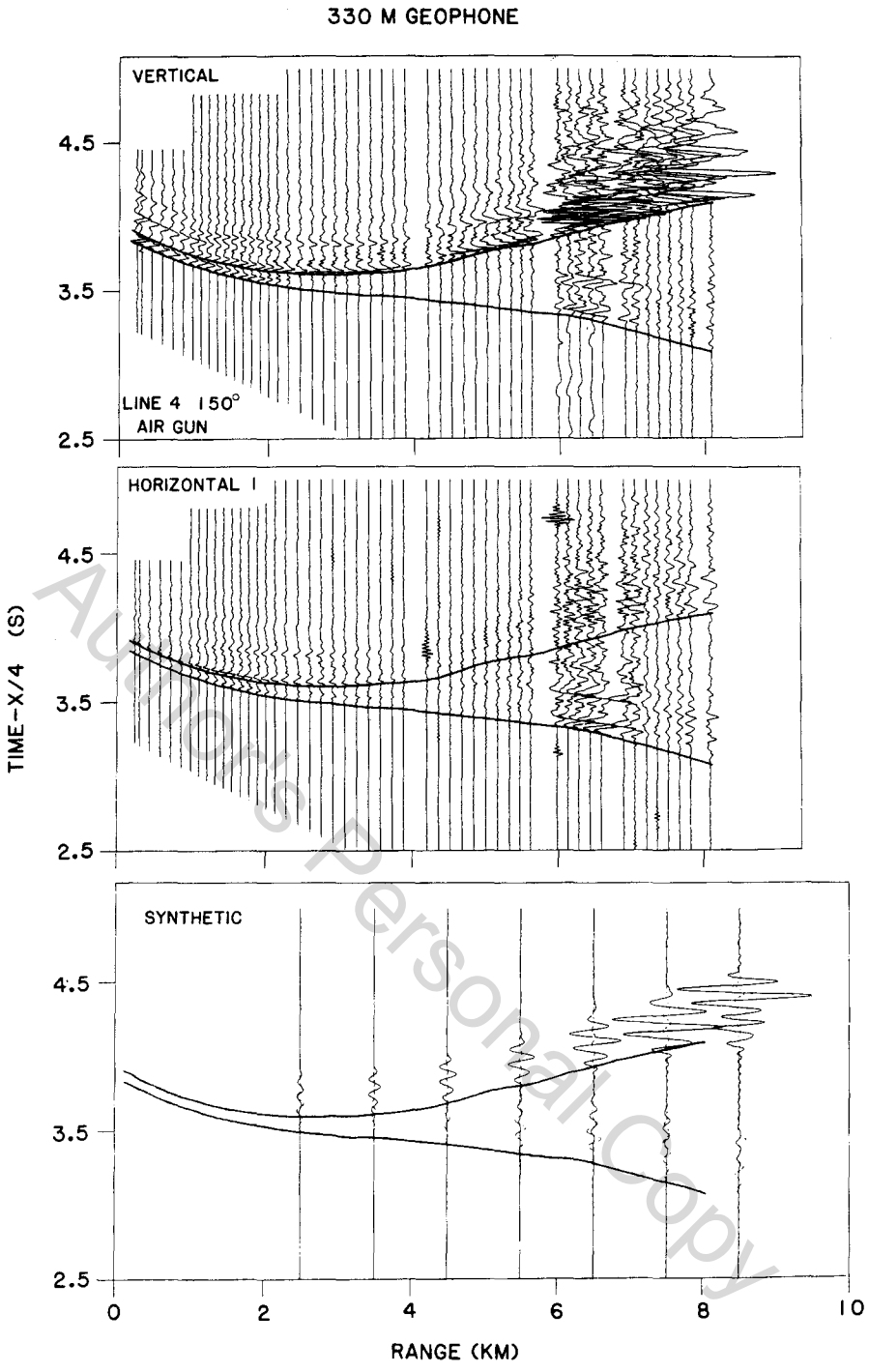

Figure 8. Comparison of traveltime and amplitude vs. range data for shot line 4 with the seismometer clamped 330-m within the basement and synthetic seismograms generated for the same line, assuming $V_s = 0.55V_p$. Synthetic vertical component is solid, horizontal is dashed. Observed seismograms corrected for geometric spreading and band-pass filtered at 5–50 Hz.

the OSE (4.6 to 5.0 km/s, depending on the propagation direction).

5. On average, the upper 0.5 km of the crust at Site 418 now consists of about 86% basalt, 9% palagonite and clay, and 5% open cracks filled with water. Of the basalts, 69% consist of pillow basalts, 27% are massive basalts, and 4% consist of cemented basalt breccias. The basalts themselves contain considerable primary (vesicular and grain boundary) porosity, bringing the total formation porosity to 15%.

6. The upper levels of the section (Unit 5 and Subunit 6A) display a higher total porosity (20%, of which 14% is primary porosity and 6% is fracture porosity) and a much higher clay content (19%) than the section as a whole. From the original core descriptions, it is clear that most of the alteration products fill pre-existing interpillow voids and fractures. Thus, the original formation porosity was about 40%, much higher than it is now. Velocity-porosity systematics based on logs demonstrate that the compressional-wave velocity of this level of the crust

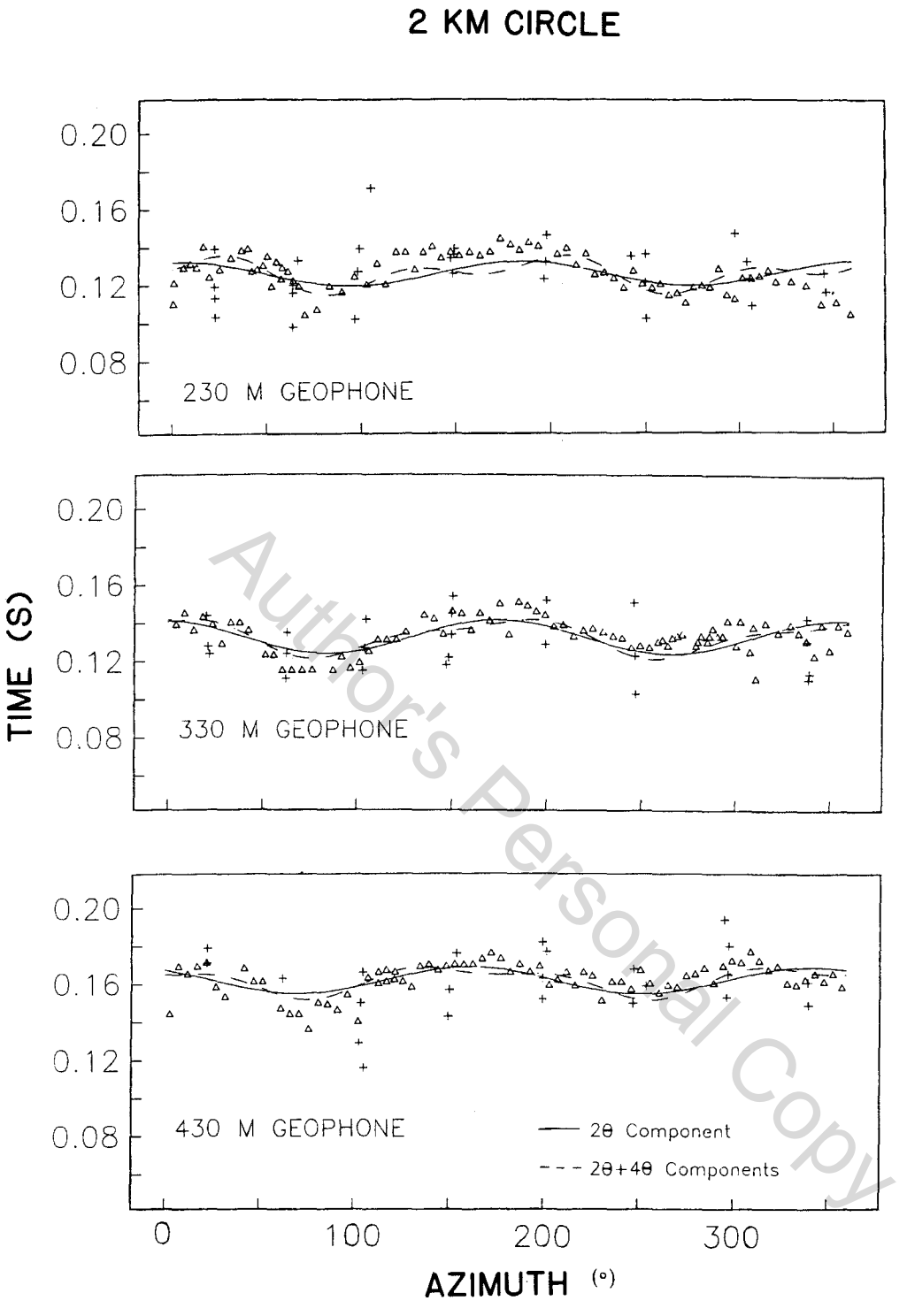

Figure 9. *P*-wave traveltimes vs. azimuth to shot points on 2-km circle (triangles) for various seismometer depths. Crosses represent arrivals from shots on radial lines within 0.3 km of circle. 2θ and 4θ components represent variations with 180° and 90° periodicities, respectively.

prior to infilling (i.e., when it resided at the ridge crest) was about 3.5 km/s, equivalent to that of Layer 2A.

7. The disappearance of Layer 2A and the pronounced changes in geophysical properties that occur with age in the upper levels of the crust are due to the infilling of voids and cracks by secondary minerals formed by rock-seawater interaction. The sequence at Site 418 is ordered and continuous, starting with Fe oxide-hydroxides and proceeding through K-rich to K-poor clays, pyrite, and finally calcite, suggesting evolution in a closed system. Because similar sequences are observed in other ODP holes, we conclude that the aging phenomena documented at Site 418 are widespread in old oceanic crust.

ACKNOWLEDGMENTS

We wish to thank the Captains and crews of the *JOIDES Resolution* and the R/V *Fred H. Moore* for their assistance during the logging and

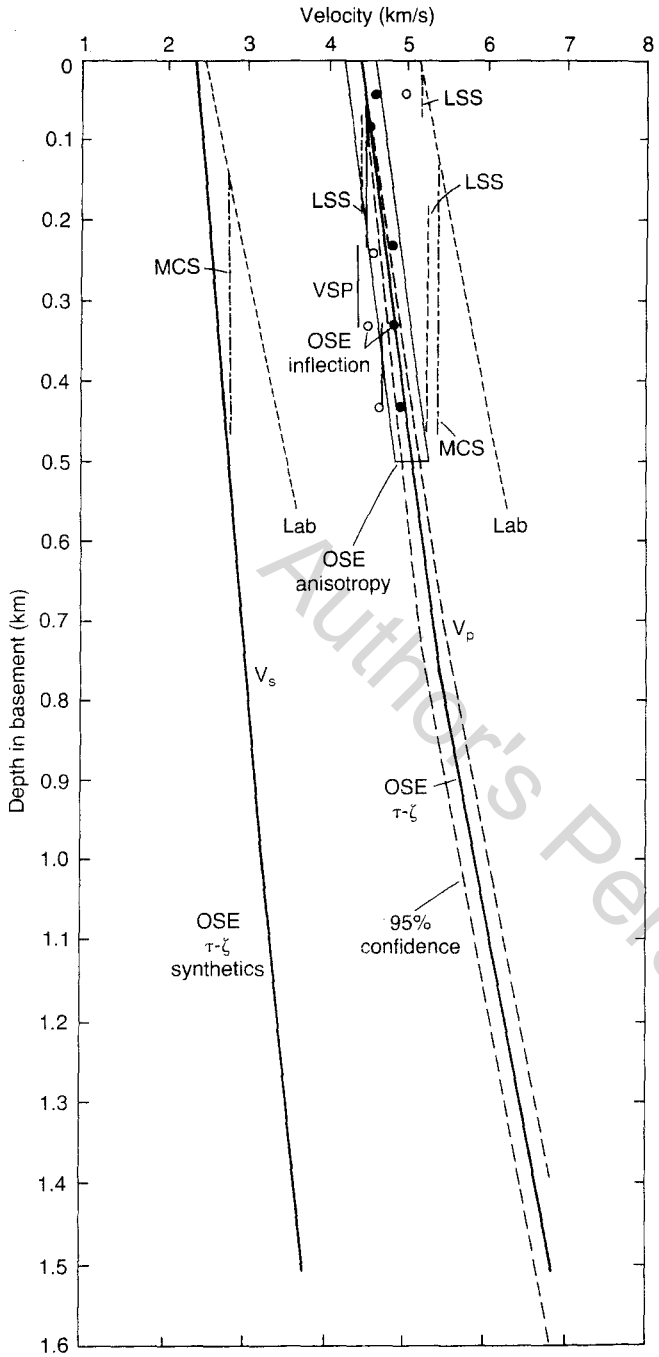

Figure 10. Comparison of compressional- and shear-wave velocities obtained in Hole 418A from laboratory studies, logging, and the oblique seismic experiment (OSE). Laboratory V_p and V_s trends represent least-squares fits to data obtained at a differential confining pressure of 0.1 kbar. Multichannel sonic (MCS) logging data from Moos (this volume); long-spaced sonic (LSS) data from Broglia and Moos (this volume). OSE data (VSP, inflection, $\tau - \zeta$, anisotropy) from Swift and Stephen (this volume); solid and open circles represent inflection point data before and after reduction to basement, respectively.

OSE; Glen Foss and Bob Caldow for their careful orchestration of rig-floor operations; Jeff Skelly of Schlumberger, Ltd., and Ewald Meyer of BGR for running the logs; Michael Reitmeyer, Daniel Larson, Patrick Thompson, and Warren Witzell for preparing and maintaining the tools; and Mark Weiderspahn and William Robinson for preparing and writing the digital acquisition system for the borehole seismometer experiment.

This study was supported by grants to R. A. Stephen from the U.S. National Science Foundation in support of the OSE (OCE-8416633), to M. H. Salisbury from Petro-Canada and the Natural Sciences and Engineering Research Council in support of logging research (IRC 8403), and to N. I. Christensen from the U.S. Navy in support of laboratory velocity studies (ONR Contract N-0001 4-84-K-0207). Grants from the U.S. Scientific Advisory Committee to the U.S. participants on the *JOIDES Resolution* supported participation on Leg 102 and post-cruise data analysis.

REFERENCES

Christensen, N. I., Blair, S. C., Wilkens, R. H., and Salisbury, M. H., 1980. Compressional wave velocities, densities and porosities of basalts from Holes 417A, 417D and 418A, Deep Sea Drilling Project Legs 51 through 53. *In* Donnelly, T., Francheteau, J., Bryan, W., Robinson, P., Flower, M., Salisbury, M., et al., *Init. Repts. DSDP*, 51, 52, 53, Pt. 2: Washington (U.S. Govt. Printing Office), 1467–1472.

Donnelly, T., Thompson, G., and Salisbury, M., 1980. The chemistry of altered basalts at Site 417, Deep Sea Drilling Project Leg 51. *In* Donnelly, T., Francheteau, J., Bryan, W., Robinson, P., Flower, M., Salisbury, M., et al., *Init. Repts. DSDP*, 51, 52, 53, Pt. 2: Washington (U.S. Govt. Printing Office), 1319–1330.

Dorman, L. M., and Jacobson, R. S., 1981. Linear inversion of body wave data, Part 1: Velocity structure from travel times and ranges. *Geophysics*, 46:138–151.

Flower, M., Ohnmacht, W., Robinson, P., Marriner, G. and Schminke, H.-U., 1980. Lithologic and chemical stratigraphy at Deep Sea Drilling Project Sites 417 and 418. *In* Donnelly, T., Francheteau, J., Bryan, W., Robinson, P., Flower, M., Salisbury, M., et al., *Init. Repts. DSDP*, 51, 52, 53, Pt. 2: Washington (U.S. Govt. Printing Office), 939–956.

Fuchs, K., and Müller, G., 1971. Computation of synthetic seismograms with the reflectivity method and comparison with observations. *Geophys. J. R. Astron. Soc.*, 23:417–433.

Hamano, Y., 1980. Physical properties of basalts from Holes 417D and 418A. *In* Donnelly, T., Francheteau, J., Bryan, W., Robinson, P., Flower, M., Salisbury, M., et al., *Init. Repts. DSDP*, 51, 52, 53, Pt. 2: Washington (U.S. Govt. Printing Office), 1457–1466.

Houtz, R., and Ewing, J., 1976. Upper crustal structure as a function of plate age. *J. Geophys. Res.*, 81:2490–2498.

Humphris, S. E., Thompson, R. N., and Marriner, G. F., 1980. The mineralogy and geochemistry or basalt weathering, Holes 417A and 418A. *In* Donnelly, T., Francheteau, J., Bryan, W., Robinson, P., Flower, M., Salisbury, M., et al., *Init. Repts. DSDP*, 51, 52, 53, Pt. 2: Washington (U.S. Govt. Printing Office), 1201–1218.

Hyndman, R. D., Salisbury, M. H., et al., 1984. *Init. Repts. DSDP*, 78B: Washington (U.S. Govt. Printing Office).

Johnson, D. M., 1980. Fluid permeability of oceanic basalts. *In* Donnelly, T., Francheteau, J., Bryan, W., Robinson, P., Flower, M., Salisbury, M., et al., *Init. Repts. DSDP*, 51, 52, 53, Pt. 2: Washington (U.S. Govt. Printing Office), 1473–1478.

Juteau, T., Noack, Y., Whitechurch, H., and Courtois, C., 1980. Mineralogy and geochemistry of alteration products in Holes 417A and 417D basement samples (Deep Sea Drilling Project Leg 51). *In* Donnelly, T., Francheteau, J., Bryan, W., Robinson, P., Flower, M., Salisbury, M., et al., *Init. Repts. DSDP*, 51, 52, 53, Pt. 2: Washington (U.S. Govt. Printing Office), 1273–1298.

Kirkpatrick, R. J., 1979. Results of downhole geophysical logging Hole 396B, DSDP Leg 46. *In* Dmitriev, L., Heirtzler, J., et al., *Init. Repts. DSDP*, 46: Washington (U.S. Govt. Printing Office), 401–408.

Leg 109 Shipboard Scientific Party, 1986. Coring the crust and the mantle. *Nature*, 323:492–493.

Levi, S., 1980. Paleomagnetism and some magnetic properties of basalts from the Bermuda Triangle. *In* Donnelly, T., Francheteau, J., Bryan, W., Robinson, P., Flower, M., Salisbury, M., et al., *Init. Repts. DSDP*, 51, 52, 53, Pt. 2: Washington (U.S. Govt. Printing Office), 1363–1378.

Levi, S., Bleil, U., Smith, B. M., and Rigotti, P., 1980. Compilation of paleomagnetic and rock magnetic results of basalt samples from Deep Sea Drilling Project Legs 51, 52, and 53. *In* Donnelly, T., Francheteau, J., Bryan, W., Robinson, P., Flower, M., Salisbury. M., et al., *Init. Repts. DSDP*, 51, 52, 53, Pt. 2: Washington (U.S. Govt. Printing Office), 1337–1350.

Newmark, R. L., Anderson, R. N., Moos, D., and Zoback, M. D., 1985. Sonic and ultrasonic logging of Hole 504B and its implications for the structure, porosity and stress regime of the upper 1 km of the oceanic crust. *In* Anderson, R. N., Honnorez, J., Becker, K., et al., *Init. Repts. DSDP*, 83: Washington (U.S. Govt. Printing Office), 479–510.

Pertsev, N. N., and Rusinov, V. L., 1980. Mineral assemblages and processes of alteration in basalts at Deep Sea Drilling Project Sites 417 and 418. *In* Donnelly, T., Francheteau, J., Bryan, W., Robinson, P., Flower, M. Salisbury, M., et al., *Init. Repts. DSDP*, 51, 52, 53, Pt. 2: Washington (U.S. Govt. Printing Office), 1219–1242.

Pritchard, R. G., 1980. Alteration of basalts from Deep Sea Drilling Project Legs 51, 52 and 53, Holes 417A and 418A. *In* Donnelly, T., Francheteau, J., Bryan, W., Robinson, P., Flower, M., Salisbury, M., et al., *Init. Repts. DSDP*, 51, 52, 53, Pt. 2: Washington: (U.S. Govt. Printing Office), 1185–1200.

Rabinowitz, P. D., Hoskins, H., and Asquith, S. M., 1980. Geophysical site summary results near Deep Sea Drilling Project Sites 417 and 418 in the Central Atlantic Ocean. *In* Donnelly, T., Francheteau, J., Bryan, W., Robinson, P., Flower, M., Salisbury, M., et al., *Init. Repts. DSDP*, 51, 52, 53, Pt. 1: Washington (U.S. Govt. Printing Office), 629–669.

Robinson, P. T., Flower, M.F.J., Swanson, D. A., and Staudigel, H., 1980. Lithology and eruptive stratigraphy of Cretaceous oceanic crust, western Atlantic Ocean. *In* Donnelly, T., Francheteau, J., Bryan, W., Robinson, P., Flower, M., Salisbury, M., et al., *Init. Repts. DSDP*, 51, 52, 53, Pt. 2: Washington (U.S. Govt. Printing Office), 1535–1555.

Salisbury, M. H., Donnelly, T. W., and Francheteau, J., 1980a. Geophysical logging in Deep Sea Drilling Project Hole 417D. *In* Donnelly, T., Francheteau, J., Bryan, W., Robinson, P., Flower, M., Salisbury, M., et al., *Init. Repts. DSDP*, 51, 52, 53, Pt. 1: Washington (U.S. Govt. Printing Office), 705–714.

Salisbury, M. H., Stephen, R., Christensen, N. I., Francheteau, J., Hamano, Y., Hobart, M., and Johnson, D., 1980b. The physical state of the upper levels of Cretaceous oceanic crust from the results of logging, laboratory studies and the oblique seismic experiment at Deep Sea Drilling Project Sites 417 and 418. *In* Donnelly, T., Francheteau, J., Bryan, W., Robinson, P., Flower, M., Salisbury, M., et al., *Init. Repts. DSDP*, 51, 52, 53, Pt. 2: Washington (U.S. Govt. Printing Office), 1579–1597.

Schreiber, E., and Fox, P. J., 1976. Compressional wave velocities and mineralogy of fresh basalts from the FAMOUS area and the Oceanographer Fracture Zone and the texture of Layer 2A of the oceanic crust. *J. Geophys. Res.*, 81:4071–4076.

Shipboard Scientific Parties, 1980a. Site 417. *In* Donnelly, T., Francheteau, J., Bryan, W., Robinson, P., Flower. M., Salisbury. M., et al., *Init. Repts. DSDP*, 51, 52. 53, Pt. 1: Washington (U.S. Govt. Printing Office), 23–350.

_____, 1980b. Site 418. *In* Donnelly, T., Francheteau, J., Bryan, W., Robinson, P., Flower, M., Salisbury, M., et al., *Init. Repts. DSDP*, 51, 52. 53, Pt. 1: Washington (U.S. Govt. Printing Office), 351–626.

Shipboard Scientific Party, 1979a. Site 395: 23°N, Mid-Atlantic Ridge. *In* Melson, W. G., Rabinowitz, P. D., et al., *Init. Repts. DSDP*, 45: Washington (U.S. Govt. Printing Office), 131–264.

_____, 1979b. Holes 396A and 396B. *In* Dmitriev, L., Heirtzler, J., et al., *Init. Repts. DSDP*, 46: Washington (U.S. Govt. Printing Office), 15–86.

_____, 1986. Site 418: Bermuda Rise. *In* Salisbury, M. H., Scott, J. H., et al., *Proc. ODP, Init. Repts.*, 102: College Station, TX (Ocean Drilling Program), 95–235.

Stephen, R. A., and Harding, A. J., 1983. Travel time analysis of borehole seismic data. *J. Geophys. Res.*, 88:8289–8298.

Stephen, R. A., Louden, K. E., and Mathews, D. H., 1980. The oblique seismic experiment on Deep Sea Drilling Project Leg 52. *In* Donnelly, T., Francheteau, J., Bryan, W., Robinson, P., Flower, M., Salisbury, M., et al., *Init. Repts. DSDP*, 51, 52, 53, Pt. 1: Washington (U.S. Govt. Printing Office), 675–704.

Date of initial receipt: 7 July 1987
Date of acceptance: 4 January 1988
Ms 102B-123